-RESEARCH PAPER-

International Journal of Mining and Geo-Engineering

IJMGE

IJMGE 57-3 (2023) 251-258

DOI: 10.22059/IJMGE.2023.352685.595014

Using magnetic data for estimating the location of lateral boundaries and the depth of the shallow salt dome of Aji-Chai, East Azerbaijan Province, Iran

Ahmad Alvandi [a, b,*], Reza Ghanati [b]

[a] *Institute of Geophysics, University of Tehran, Tehran, Iran.*

[b] *University of Applied Science and Technology (UAST), Hamedan Province Branch, Hamedan, Iran.*

Article History:

Received: 19 December 2022.

Revised: 11 April 2023.

Accepted: 07 May 2023.

ABSTRACT

Magnetic data play a significant role in the interpretation of various geologic structures using depth estimation methods and edge detection filters. In this study, we applied methods based on directional derivatives, such as tilt-depth (TD), signum transform (ST), source distance (SD), and classical Euler deconvolution (ED) to estimate the depth of the magnetic sources. Moreover, to enhance the edges of magnetic field anomalies, we utilized the total horizontal derivative (THD), analytical signal (AS), tilt angle (TA), theta map (TM), hyperbolic tilt angle (HTA), the tilt angle of horizontal derivative (TAHG), and logistic function of total horizontal gradient (LTHD). These algorithms were tested on a synthetic magnetic model with noise and noise-free data to understand their performance. Since the edge detection filters are sensitive to noise, we carried out an upward continuation (UC) filter before the reduction of data to the magnetic pole to reduce the noise effect. After comparing the efficiency of the approaches in estimating the depth and horizontal lateral boundaries, these methods were applied to the data surveyed from the Aji-Chai salt dome in East Azerbaijan Province, Iran. The results obtained from the depth determination methods were compared with the drilling report from Iran's geological survey and the three-dimensional classical Euler deconvolution method.

Keywords: *Aji-Chai salt dome, Depth estimation methods, Edge detection filters, Magnetic data.*

1. Introduction

Magnetic surveying is a common and old geophysical method used to explore near-surface envi-ronments in a non-destructive manner. Enhancing data quality,, reducing noise, and developing computer programs have led to the creation of higher derivative computational methods that can quickly and accurately analyze geologic structures. Estimating the edges of buried geological structures can help the interpreter in providing a suitable and high-quality interpretation. The edge detection filters are combinations of horizontal and vertical magnetic gradients. These filters can efficiently examine magnetic maps and estimate the location of lateral boundaries of magnetic anomalies. Some of these filters include the total horizontal derivative [1], the analytic signal [2], the tilt angle [3]; the theta map [4]; the hyperbolic tilt angle [5], and the tilt angle of the horizontal derivative [6]. Pham et al. (2019) introduced the logistic function of the total horizontal gradient high resolution filter to estimate the edges of magnetic sources. It has better accuracy in detecting the boundaries of potential field sources [7, 8, 9]. Another important parameter in determining the characteristics of magnetic anomalies is depth. In recent years, many effective depth estimation methods have been introduced based on the horizontal and vertical derivatives of the potential field data [10]. These methods are classified into automatic and semi-automatic categories and are useful methods for interpreting magnetic data. Salem et al. (2007) introduced the tilt-depth method based on the concept of the tilt-angle edge detection filter for magnetic anomalies [11]. The Signumtransformation is another method based on simple derivative used for qualitative and quantitative interpretation of magnetic sources [12]. De Souza and Ferreira (2015) calculated the automatic depth of magnetic anomalies using the Signum function [12, 13]. The analytical signal is another popular filter for determining the edges and depth of magnetic structures. Accordingly, many methods use the analytical signal amplitude to interpret potential field data. Cooper (2015) introduced a source distance method based on the analytical signal approach to estimate the depth of anomalies through reduction to pole (RTP) of magnetic data [14]. Despite the recent development of various algorithms for magnetic sources depth estimation and edge detection, it might be still wothwhile to further demonsterate pros and cons of such methods. Hence, the main purpose of this study is to investigate and compare some methods for determining the depth and edges of magnetic anomalies based on the directional derivatives of the magnetic field, which have been widely used in recent years. Also, the best method for calculating the depth and edges of buried structures among those used in this article will be introduced. This study investigates synthetic models with noise and noise-free to evaluate the applicability of the mentioned methods. Finally, we implement the proposed methods to the magnetic data of the Aji-Chai salt dome, and a new geological map with horizontal lateral boundaries for the Aji-Chai is constructed using the obtained information. It should be considered that in subsequent studies, standard methods can be employed for determining the depth and horizontal position of buried structures ,also for inverse modelling [10, 23] with correct initial assumptions [20].

* Corresponding author: *E-mail address:* aalvandi@ut.ac.ir (A. Alvandi).

2. Methods for Depth and Edge Determination

2.1. Edge Detection Algorithms

In this study, we take advantage of the total horizontal gradient (THD), total gradient (or analytic signal (AS)), tilt angle (TA), hyperbolic tilt angle (HTA), theta map (TM), the tilt angle of horizontal derivative (TAHG), and the logistic function of horizontal gradient (LTHD) as edge detection methods. Table 1 briefly states the expressions for these methods.

In Table (1), ∂M/∂x, ∂M/∂y and ∂M/∂z are the derivatives of the magnetic field in x, y, and z directions, respectively. This research assumes a value of 2 for α in all synthetic and real models.

2.2. Depth calculation methods

The following describes the methods used to estimate the depth of magnetic anomalies, including the tilt depth (TD), signum transform (ST), source distance (SD), and standard (classical) Euler deconvolution (ED) techniques used and compared in this study.

2.2.1. Tilt-Depth (TD)

Salem et al. (2007) proposed the TD method for the interpretation of magnetic anomalies. In Equation (3), the value of the tilt angle changes in the range of ± 90°. This value becomes positive at the top of the source and approaches zero near the edge of the source. Assuming a vertical magnetization direction i.e., RTP data for TA, a simplified equation for the tilt angle in the magnetic field can be obtained [11]:

$$TD=\tan^{-1}\left(\frac{d}{h}\right) \quad (1)$$

In Equation (1), d and h are the buried horizontal and vertical distances from the anomaly, respectively. Salem et al. (2007) have shown that the depth of the anomaly can be calculated by measuring half the distance between the countering of the 45° tilt angle of the magnetic field [11].

2.2.2. Signum Transform (ST)

de Souza and Ferreira (2015) presented the ST method, which uses the signum transform method to estimate the depth of magnetic sources with vertical magnetization i.e, RTP data. Signum transform values are expected to be 1 over the sources and -1 outside the sources. Assuming a vertical magnetization direction, the depth of the anomaly is calculated according to the following relationships:

$$h = \frac{x_v^2 - x_{vh}^2}{2x_{vh}} \quad (2)$$

where x_v and $x_{vh}$are the zero-crossover points for the first-order vertical derivative and the first-order vertical derivative minus the total horizontal derivative, respectively. The input parameter of Equation 2 is obtained from the signum transformed anomalies [12].

Table 1. Tabulation of the various edge enhancement methods used in the present study [15, 16].

Equations	Advantages	Limitations
$THD=\sqrt{\left(\frac{\partial M}{\partial x}\right)^2+\left(\frac{\partial M}{\partial y}\right)^2}$	– The amplitude maxima is located over the edge's of the source.	– cannot equalize the amplitude of sources with different depths. – Not suitable for super imposed structurers.
$AS=\sqrt{\left(\frac{\partial M}{\partial x}\right)^2+\left(\frac{\partial M}{\partial y}\right)^2+\left(\frac{\partial M}{\partial z}\right)^2}$	– The amplitude maxima is located over the centre of the source. – Insensitive to direction of magnetization.	– Cannot equalize the amplitude of sources with different depths. – Not suitable for super imposed structures. – Unable to estimate deep and thin anomalies edge.
$TA=\tan^{-1}\frac{\frac{\partial M}{\partial z}}{\sqrt{\left(\frac{\partial M}{\partial x}\right)^2+\left(\frac{\partial M}{\partial y}\right)^2}}$	– Can equalize the amplitude of sources with different depths.	– Less effective in enhancing the edges of the deep and thin sources. – The estimated edges are not sharp.
$HTA=Re\left[\tanh^{-1}\frac{\frac{\partial M}{\partial z}}{\sqrt{\left(\frac{\partial M}{\partial x}\right)^2+\left(\frac{\partial M}{\partial y}\right)^2}}\right]$	– Can equalize the amplitude of sources with different depths at the same time.	– Draw false and spurious horizontal boundaries. – Less effective in enhancing the edges of the buried sources.
$TM=\cos^{-1}\frac{\sqrt{\left(\frac{\partial M}{\partial x}\right)^2+\left(\frac{\partial M}{\partial y}\right)^2}}{\lvert AS\rvert}$	– The amplitude minimum is located over the edge's of the source.	– Draw false and spurious horizontal boundaries. – Less effective in enhancing the edges of the deep and thin sources.
$TAHG=\tan^{-1}\frac{\frac{\partial THD}{\partial z}}{\sqrt{\left(\frac{\partial THD}{\partial x}\right)^2+\left(\frac{\partial THD}{\partial y}\right)^2}}$	– The amplitude maxima is located over the edge of the source – Can balance the edges with sources located at different depths at the same time.	– The images resolution is low.
$LTHD=\left[1+\exp\left(-\frac{\frac{\partial THD}{\partial z}}{\sqrt{\left(\frac{\partial THD}{\partial x}\right)^2+\left(\frac{\partial THD}{\partial y}\right)^2}}\right)\right]^{-\infty}$	– Can balance the edges with sources located at different depths at same. – The amplitude maxima is located over the edge of the sources. – The images have a good resolution. – does not create a false and spurious edges.	

2.2.3. Signum Transform (ST)

Cooper (2015) introduced the SD method using the analytical signal amplitude filter to estimate the depth of magnetic sources, where the depth of the magnetic source is calculated via:

$$R_{AS} = \frac{AS_0}{AS} = h \quad (3)$$

where

$$AS_0 = \sqrt{H_x(M)^2 + H_y(M)^2 + M^2} \quad (4)$$

AS_0 is the zero-order analytic signal amplitude and $H_x(M)$ and $H_y(M)$ are the Hilbert transform of the magnetic field in the x and y directions. h has its minimum value directly over the anomaly, and at that point h is then equal to the depth to the top of the causative source [14].

2.2.4. Euler deconvolution (ED)

Reid et al. 1990 presented the Euler deconvolution semi-automatic method using Euler's theorem for homogeneous functions to estimate the depth of magnetic sources, resulting in a simplified equation for ED [21, 22]:

$$(x - x_0)\frac{\partial M}{\partial x} + (y - y_0)\frac{\partial M}{\partial y} + (z - z_0)\frac{\partial M}{\partial z} = -N(M - F) \quad (5)$$

where x_0, y_0, z_0 are the buried source locations; F is the regional value of the total field, and N is the structural index (SI) and has different values for different types of sources in magnetometry (sphere=3; vertical cylinder =2; horizontal cylinder=1; dike=1; contact, and step=0).

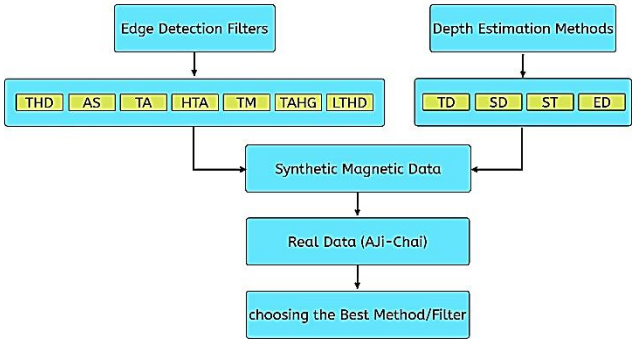

Fig 1. Flowchart used for estimating depth and edge location of the magnetic sources.

3. Application to the synthetic model

In this section, we test the performance of the edge detection and depth estimation methods on a synthetic model (Fig. 2). The 2D and 3D models of the synthetic data are shown in Figure (2). The parameters of the model are also described in Table (2). Figure 2a contains two prismatic bodies (A and C) with the same susceptibility but varying sizes and depths, and three sources (B, D, and E) of different depths and sizes. The synthetic model with positive and negative susceptibility is made on a regular grid of 10000 m×10000 m in the north-south and east-west directions with a sample spacing of 100 m. The magnetic anomaly map and the results obtained using different edge detection filters, including total horizontal gradient, analytical signal, tilt angle, hyperbolic tilt angle, theta map, tilt angle of horizontal derivative, and logistic functionof the horizontal gradient are shown in Figure (3).

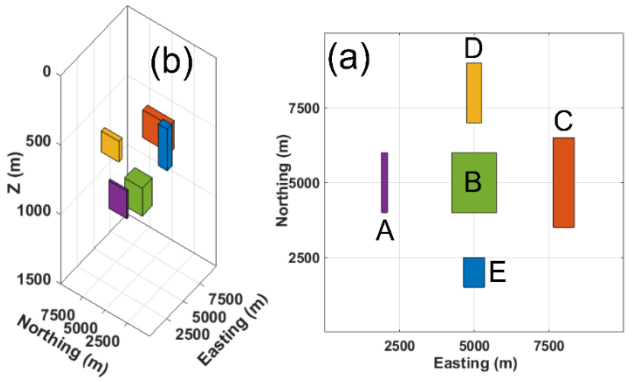

Fig 2. a) Plan view of the synthetic model, b) 3D view of the synthetic model from (a).

Table 2: Susceptibility and geometry parameters of the synthetic model.

Parameters/Model label	A	B	C	D	E
X-coordinates of center (m)	2000	5000	8000	5000	5000
Y-coordinates of center (m)	5000	5000	5000	8000	2000
Width (m)	200	1500	700	500	700
Thickness (m)	200	200	200	150	300
Inclination(°)	90	90	90	90	90
Declination (°)	0	0	0	0	0
Susceptibility (SI)	0.001	-0.003	0.001	0.002	0.003
Depth (m)	600	700	400	500	200

Figure 3a shows the magnetic anomaly of the synthetic model. İn addition, Figures 3b and c show the horizontal lateral boundaries of the synthetic magnetic model in Figure 3a outlined using the THD and AS filters, respectively. As can be seen, the filters are dominated by the shallow body (prism E), while the deeper bodies (prism A, B, C, and D) are blurred. Figure 3d depicts the result of applying the filter TA. Although the edges of five prisms (A, B, C, D, and E) are outlined by zero contours, the false contours between the sources make interpretation difficult. Figure 3e shows the edges of the synthetic model using the HTA filter with the maximum amplitude values. Although the boundaries of the deep and shallow structures are defined simultaneously, the generation of negative boundaries around the sources complicates the interpretation of the output image. Figure 3f shows the result obtained by applying the TM filter to the data in Figure 3a. The minimum amplitude values of TM show the edges of the shallow and deep sources at the same time but produce false borders between the bodies, making the interpretation of the map difficult. Figure 3g and 3h show the TAHG and LTHD filters, respectively. The TAHG and LTHD filters are able to balance all weak and large amplitudes and also avoid generating false edges. However, the LTHD filter provides a higher resolution compared to the TAHG filter. Since the edge detection filters are based on the derivative of the data, they may amplify the noisy signals in the data. Therefore, the ability of the filters for noisy data was investigated. Fig. 4a shows the magnetic anomaly due to the five prisms with the addition of 5% random noise in order to test the effect of noise on the synthetic magnetic model. The results of using the different edge detection filters including (THD), (AS), (TA), (HTA), (TM), (TAHG), and (LTHD) are shown in Figure (4b-h).THD and AS are dominated by the large amplitude responses of shallow prisms (E), while the responses of deeper prisms (A, B, C and D) are not clear. The TA, HTA, and TM filters are sensitive to noise and the lateral boundaries of thin and deep

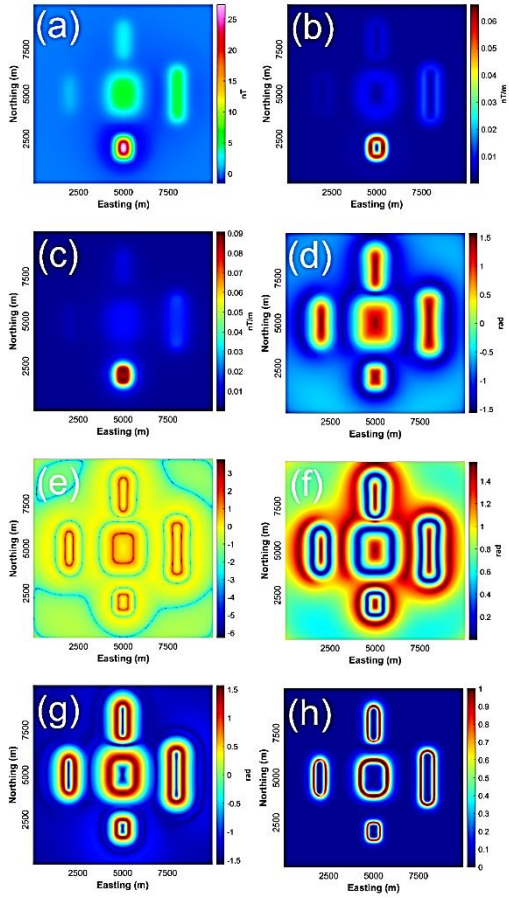

Fig 3. a) Magnetic anomaly map of the synthetic model. Edge detection of the synthetic model of the free noise by the filters of b) THD, c) AS, d) TA, e) HTA, f) TM, g) TAHG, h) LTHD.

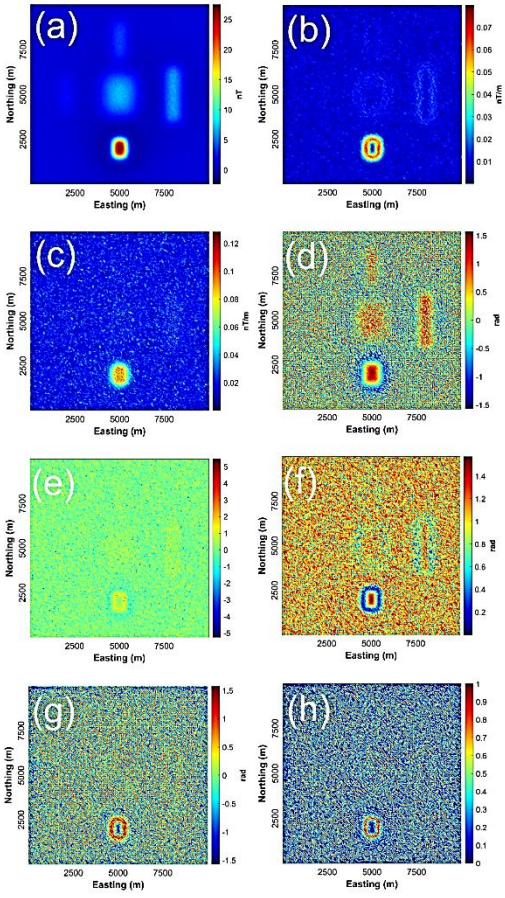

Fig 4. a) Magnetic anomaly map of the synthetic model with 5% random noise. Determination of the edge of the synthetic model with 5% random noise by the method, b) THD, c) AS, d) TA, e) HTA, f) TM, g) TAHG, h) LTHD.

sources are not clear. The TAHG and LTHD filters can define the edges of the shallow source, but the horizontal boundary of the deeper sources is not clear. Therefore, to reduce the noise effect, an upward continuation (UC) filter of 200 m is applied to the synthetic model before edge detection. THD and AS cannot equalize the edge of shallow and deep at the same time. The TA filter can equalize the edge of shallow and deep sources at the same time. The filter TA shows that the sharpness at the inner and outer edges of the sources cannot be achieved by the filter TA. In Figure 5e, the maximum amplitude of the HTA filter does not work well for thin and deep sources. TM can define the horizontal boundaries of the shallow and deep sources. However, one of the disadvantages of this method is the generation of false boundaries between buried structures. In Fig. 5g and h, it is clear that the TAHG and LTHD filters were much more successful than the others in improving the source boundaries, although the LTHD filter produces a higher resolution map than the TAHG map.

The depth values of the synthetic model prisms were calculated using the methods of tilt depth, signum transform, source distance, and standard Euler deconvolution (Fig. 6). The numerical results of the methods for determining the depth of the prisms are described in Table (3). We used the mode statistical method to calculate the depth of buried sources. The mode in a histogram figure is the value with the highest frequency. The sensitivity of the depth determination methods was investigated using synthetic data with random noise (Fig. 7). The numerical results obtained from the methods are described in table (3).

Comparing the numerical results in table (3) with the real values of the prisms' depth in table (1), we find that the TD method is suitable for both shallow and deep buried structures, and the edges are in the depth range from 200 m to 450 m.

This reduction in interpretation error aids in selecting the exact depth of the anomaly. The sensitivity of the SD and ST methods to depth is significantly high for the four deep structures A, B, C, and D. Also, it should be noted that the ST and SD methods produces spurious and false solutions around sources A, B, C, D, and E. In noisy cases, the TD method is more stable. The range of depth variations is from 100 m to 1000 m, and the depths of deep and shallow prisms are specified separately. The SD method is more sensitive to noise, the depth is set between 100 m and 1000 m, and in this case, the depth of prisms is estimated between 100 m and 200 m. Besides, the results obtained from the ST depth calculation method indicate the inaccuracy of this method in determining the depth of buried structures. The ED method also has reasonable accuracy in determining the depth of buried structures, as shown in Figures 6 and 7 and supported by the numerical results in Table 2. This approach confirms the accuracy of the TD method in determining the depth of magnetic anomalies.

4. Application to the RTP anomaly in the Aji-chai region

4.1. Geological Setting

The Aji-Chai region is located in the middle south (north of Mahneshan) of East Azerbaijan Province and is marked on the geological map at a scale of 1:100,000 [17]. This area includes marl, sandstone, and conglomerate sediments along with evaporite sediments, which have been exposed to strong erosion due to their loose nature, forming a low morphology with shallow valleys. These salt domes are located in the tectonic structural zone of the Central Iran and in the upper red formation of the middle to upper Miocene period. The salt domes in the Azerbaijan province are generally small in volume. They

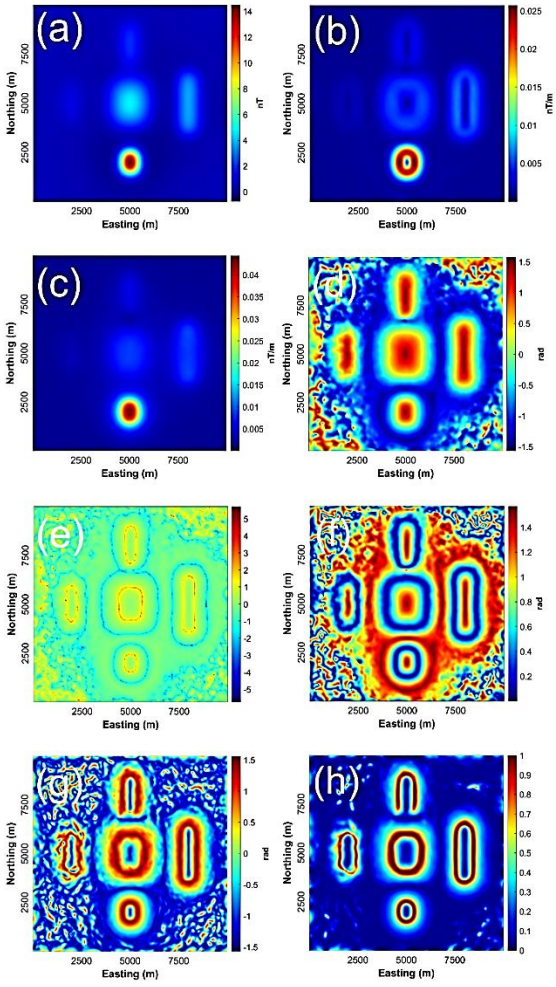

Fig 5. a) Magnetic anomaly map of the synthetic model with upward continuation of 200 m, b) THD, c) AS, d) TA, e) HTA, f) TM, g) TAHG, h) LTHD.

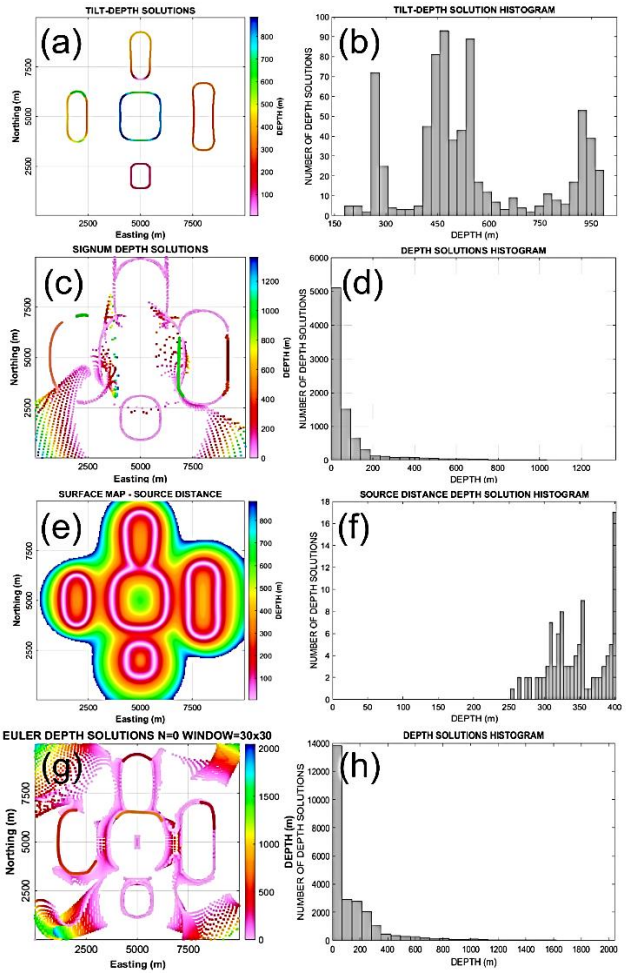

Fig 6. Depths obtained with the three-dimensional methods for the synthetic magnetic model: (a) the TD method, (b) The histogram of the evaluated depths corresponding to figure 6a; (c) the ST method, (d) The histogram of the evaluated depths corresponding to figure 6c; (e) the SD method, (f) The histogram of the evaluated depths corresponding to figure 6e; (g) the Classical Euler deconvolution method (structural index=0 and window size=30), (h) The histogram of the evaluated depths corresponding to figure 6g.

are located near the earth's surface and are significant in terms of potash deposits. In 2008, magnetometric surveys were carried out by the Geological Survey of Iran (GSI) in the Aji-Chai region to estimate the depth and extent of the Aji-Chai salt dome for potash exploration [17]. The study area is located between coordinates 731800E and 732400E and 4108000N and 4108600N in UTM coordinates. In the GSI report, the depth of the salt dome is estimated to rang from 30 m to 60 m. This drilling report also indicates that the primary potash source begins at a depth of 38 m [17, 18]. Figure 8(a) shows the distribution map of salt domes in Iran (Maghsoudi, 2021) and figure 8(b) shows the geological map of the Aji-Chai region [17].

The upward continuation of the RTP map (5 m) is shown in Fig. 10a. The results of using different edge enhancement filters, including (THD), (AS), (TA), (HTA), (TM), (TAHG), and (LTHD), are shown in Figures (10b-h). The approximate boundary of the salt dome is marked with a black closed line on the edge determination maps. The THD and AS maps are dominated by the large amplitudes, and other detected buried sources are blurred, making the interpretation of deep structures difficult (Figs. 10b and 10c). The TA, HTA, TM, TAHG, and LTHD maps (figs. 15d, e, f, g, and h) show strong signatures of salt dome and other structures. However, in this case, the structural horizontal lateral bondaries cannot be clearly identified using the TA, HTA, and TM filters. TAHG and LTHD are powerful methods that simultaneously balance small and large amplitude signals (Figs. 10g and 10h). Fig. 10h shows the results of applying the LTHD approach to the Aji-Chai magnetic dataset. The LTHD filter balances the amplitudes of large and

Table 3: Results of estimating the depth of the synthetic model using TD, ST, SD, and ED methods.

Methods/Calculated top Depth (m) Values									
	Label	TD	%Error	ST	%Error	SD	%Error	ED	%Error
Free noise	A	450	25	600	0	100	83	600	0
	B	700	0	400	75	100	85	500	28
	C	400	0	100	75	100	75	300	25
	D	400	25	100	80	100	80	250	50
	E	200	0	100	50	100	50	200	0
with noise	A	500	16	null	-	100	83	600	0
	B	500	28	null	-	100	85	700	0
	C	400	0	null	-	100	75	200	50
	D	400	20	null	-	100	80	400	20
	E	200	0	null	-	100	50	200	0

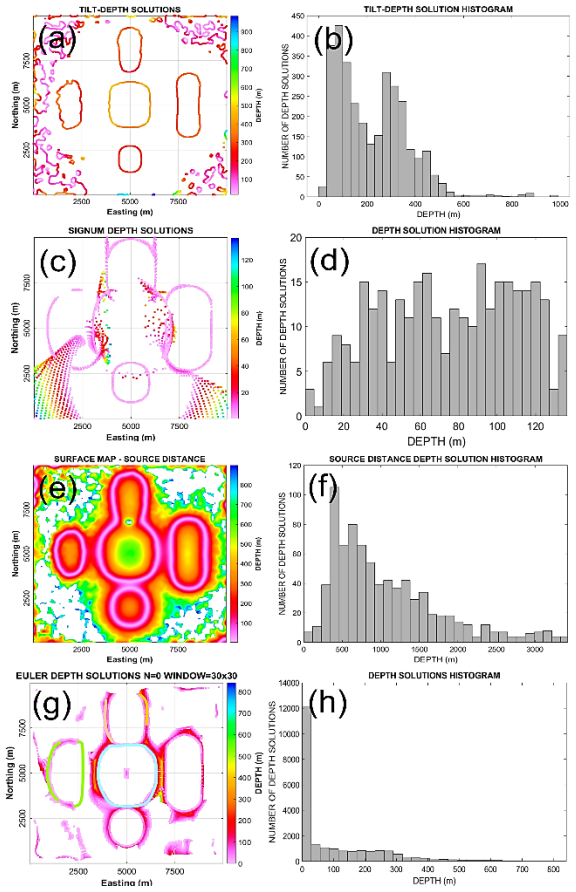

Fig 7. Depths obtained using the three-dimensional methods for the synthetic magnetic model with random noise: (a) the TD method, (b) The histogram of the evaluated depths corresponding to figure 7a; (c) the ST method, (d) The histogram of the evaluated depths corresponding to figure 7c; (e) the SD method, (f) The histogram of the evaluated depths corresponding to figure 7e; (g) the Classical Euler deconvolution method (structural index=0 and window size=30), (h) The histogram of the evaluated depths corresponding to figure 7g.

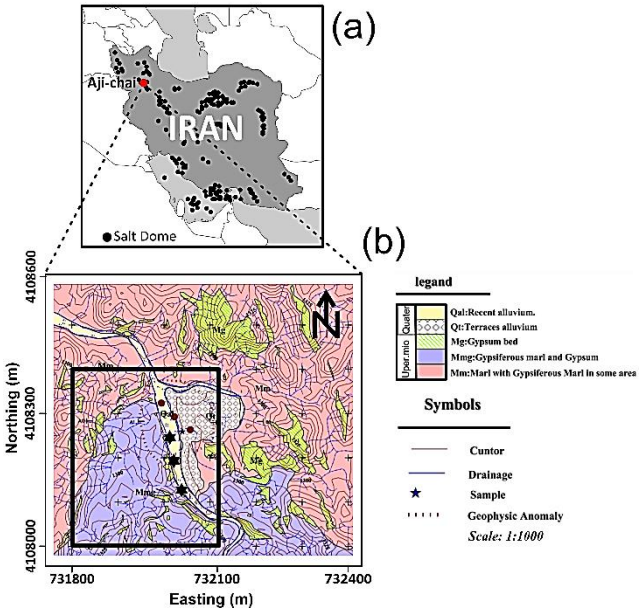

Fig 8. a) The Map of Iran and distribution of salt domes, the study area (the Aji-Chai salt dome region) in the northwestern Iran is indicated by a red dot [19]. b) The geological map of the Aji-Chai region (The range of magnetic data survey is marked with a black rectangle) [17, 18, 20].

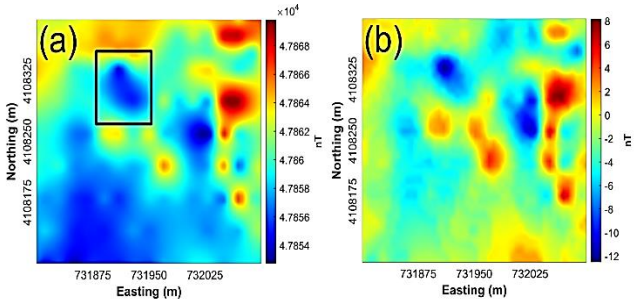

Fig 9. a) The magnetic anomaly map (the negative anomaly of the salt dome is marked with a black rectangle); b) The RTP magnetic anomaly map.

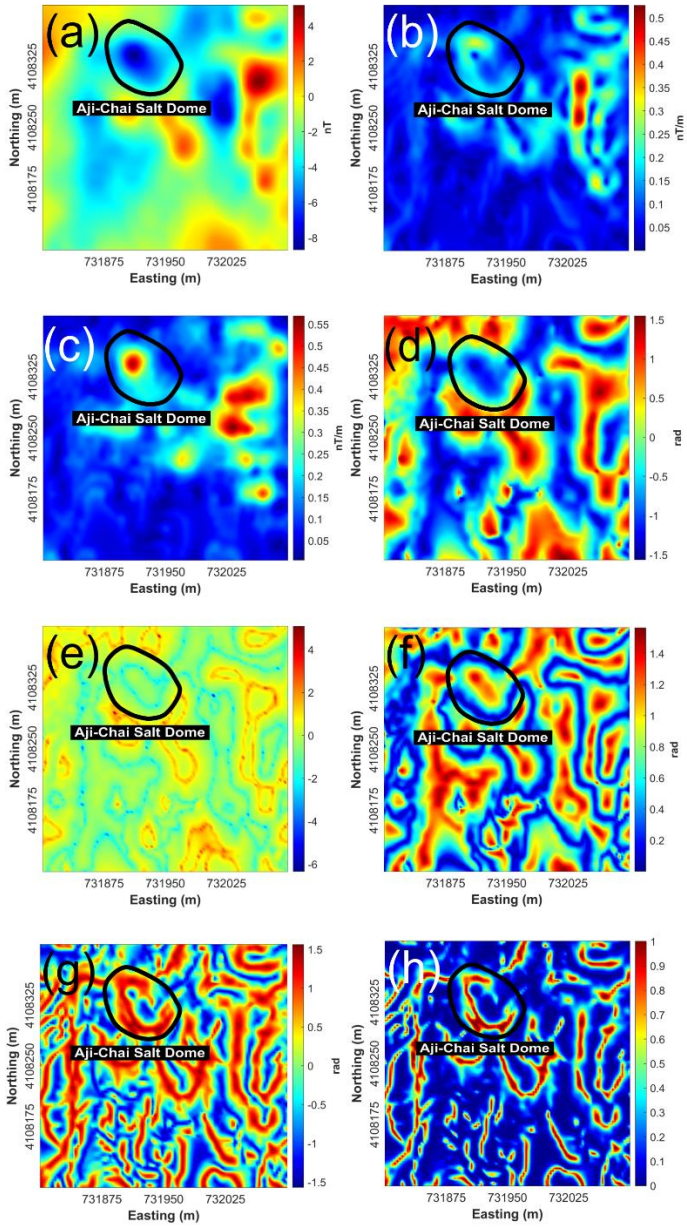

Fig 10. a) An upward continuation of the RTP map (5 m); edge detection of the salt dome using the methods: b) THD, c) AS, d) TA, e) HTA, f) TM, g) TAHG, h) LTHD.

small anomalies simultaneously and is very effective in identifying geological structures compared to the previously tested methods. The horizontal gradient logistic function is effective in determining the horizontal boundray of magnetic anomalies and removing the additional map closures. It has much higher resolution compared to other methods and is less sensitive to noise than other filters. The comparison of the obtained map with the geological map of the region by Abedi (2018) shows that other anomalies and boundaries are well identified in the LTHD map and there is a good agreement between them. The Euler's deconvolution method was introduced by Reid et al. (1990) and Thompson (1982) as a standardized and reliable method in the semi-automated interpretation of magnetic anomalies. To validate the depth determination results for the Aji-Chai salt dome, this method using the structural index and window size. was also used (Figure 11).

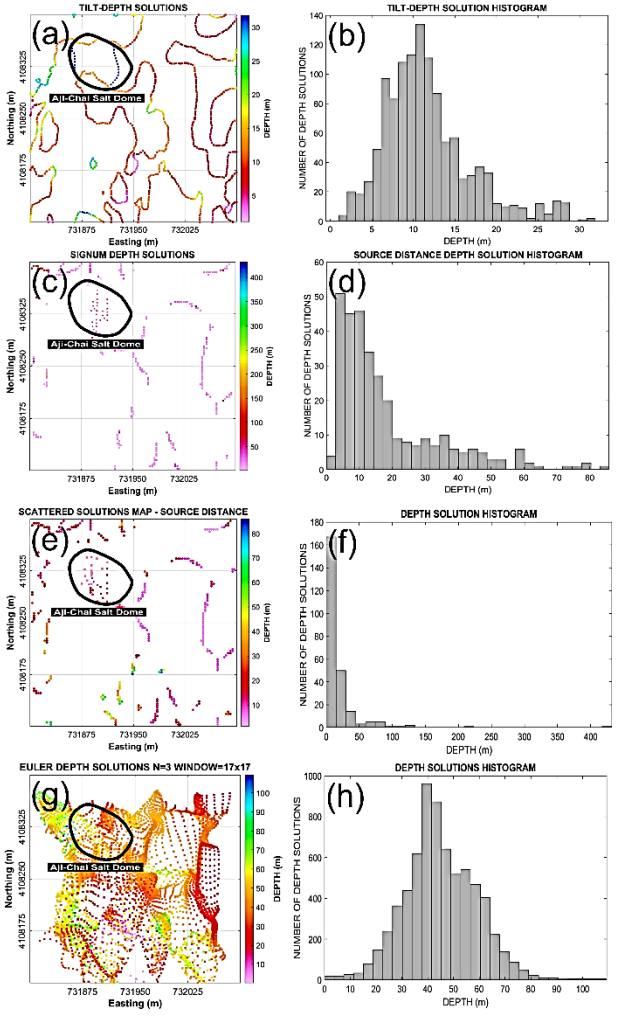

Fig 11. Depths estimated by the three-dimensional methods for the field magnetic model (The approximate boundary of the salt dome is marked with a black closed line on the depth estimation maps): (a) Method of TD, (b) The histogram of the evaluated depths corresponding to Fig. 11a; (c) the ST method, (d) The histogram of the evaluated depths corresponding to Fig. 11c; (e) the SD method, (f) The histogram of the evaluated depths corresponding to Fig. 11e. (g) of the ED method (structural index=3 and window size =17), (h) The histogram of the evaluated depths corresponding to Fig. 11g.

The numerical results of the depth determination methods of TD, ST, SD, and ED are described in Table (4). It can be seen that the depths estimated by the TD method generally align well with the drilling data and the 3D Euler deconvolution method , while the SD and ST methods are unreliable. Figure 11g shows the depth calculation map using the ED method. In this figure, the depth of the salt dome is greater in the eastern part and shallower in the western part. In addition, the simplified geological map of the Aji-Chai salt deposit is shown (Figure 12). This model was created using the LTHD filter map information and gelogical data by RockWorks and Surfer Golden softwares.

Table 4. Results of determining the top depth of the Aji-Chai salt dome using TD, ST, SD, and ED methods and drilling values.

Results of the determination of the Aji-Chai depth	
Method	**Depth (m)**
Tilt Depth (m)	30
Signum Transform (m)	10
Source Distance (m)	15
Euler Deconvolution	35
Drilling [17]	30

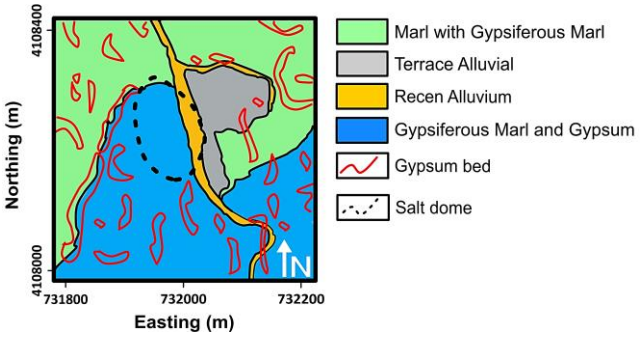

Fig. 12. The simplified geological map with horizontal lateral edges of the Aji-Chai salt deposit in the NW of Iran. The gypsum bed has been superimposed on the map (reproduced from [17]).

5. Conclusions

Interpretation of magnetic data plays an important role in determining the parameters of geologic structures. For this purpose, different edge detection filters were used to detect the horizontal position of the buried structures. The edge estimation methods used in this study, such as total horizontal derivative, analytical signal, tilt angle, theta map, hyperbolic tilt angle, tilt angle of horizontal derivative, and logistic function of total horizontal gradient logistic function, were tested on synthetic models with and without noise before being applied to the Aji-chai salt dome magnetic field data. In the real model, both the total horizontal gradient and the analytical signal filters are not able to determine the boundary of the buried structures with different depths simultaneously. Therefore, the boundary of the salt dome is not clear in these maps. Also, local phase filters such as tilt angle, theta angle, and hyperbolic tilt angle are unable to determine the exact position and lateral boundary of the Aji-chai salt dome by drawing additional boundaries or fuzzy boundaries. The LTHD and TAHG filters have defined the boundary of the salt dome. However, the logistic filter has higher quality and resolution. The results show that the quality of the collected data and the reduction of noise in the data can play an important role in creating edge determination maps. Another essential parameter that is important in the interpretation of magnetic maps is the calculation of the anomaly depth. The depth estimation methods used in this work, such as tilt-depth, signum transform, source distance, and classical Euler deconvolution, are tested on synthetic and field magnetic models. The results of the analysis of the synthetic and real data show that the tilt-depth and standard Euler deconvolution methods can accurately calculate the depth values without false solutions around

and inside the sources. In addition, the depths estimated by the automatic tilt-depth method and the semi-automatic Euler deconvolution generally agree well with the drilling data, so these methods can be used to estimate the depth of magnetic anomalies and provide reliable results. Unfortunately, due to the presence of field derivatives, the SD and ST methods are very sensitive to noise in their relationships and cannot determine the depth of the salt dome. The results of the TD and ED methods, used to estimate the depth of the anomaly, show that the depth of the anomaly (the Aji-Chai salt dome) is between 20 and 50 meters and has a spherical shape, with the highest concentration of the anomaly between 30 and 40 meters.

Acknowledgments

The authors thank the Geological Survey of Iran (GSI) for providing the geophysical data and the report, and the editor, reviewers, Dr. Hazel Deniz Toktay and Dr. Luan Thanh Pham whose assistance during the review process greatly.

Data and Materials Availability

Synthetic data associated with this research are available and can be obtained by contacting the corresponding author.

REFERENCES

[1] Cordell, L. & Grauch, V. J. S. (1985). Mapping basement magnetization zones from aeromagnetic data in the San Juan basin, New Mexico. In: Hinze W. J. (Editor). The Utility Of Regional Gravity And Magnetic Anomaly Maps, Society of Exploration Geophysics (SEG), 181–197.

[2] Roest W. R. J., Verhoef, J. & Pilkington, M. (1992). Magnetic interpretation using the 3-D analytic signal. Geophysics, 57(1), 116–125.

[3] Miller, H.G. & Singh, V. (1994). Potential fled tilt a new concept for location of potential field sources. Applied Geophysics, 32, 213–217.

[4] Wijns, C., Perez, C. & Kowalczyk, P. (2005). Theta Map: edge detection in magnetic data. Geophysics, 70, 39–43.

[5] Cooper, G. R. J. & Cowan, D.R. (2006). Enhancing potential field data using filters based on the local phase. Computers & Geosciences, 32(10), 1585-1591.

[6] Ferreira, F. J. F., de Souza, J., Bongiolo, A. B. S. & de Castro, L. G., (2013). Enhancement of the total horizontal gradient of magnetic anomalies using the tilt angle: Geophysics, 78: J33-J41.

[7] Alvandi, A., Toktay, H, D., & Pham, L, T. (2022b). Capability of improved Logistics filter in determining lateral boundaries and edges of gravity and magnetic anomalies Tuzgolu Area Turkey, Journal of Mining Engineering, 17(56), pp. 57-72. doi: 10.22034/ijme.2022.538984.1889.

[8] Eldosouky, A, M., Pham, L, T., Mohmed, H., &Pradhan, B. (2020). A comparative study of THG, AS, TA, Theta, TDX and LTHG techniques for improving source boundaries detection of magnetic data using synthetic models: a case study from G. Um Monqul, North Eastern Desert, Egypt. J. Afr. Earth Sci., 170 p. 103940, 10.1016/j.jafrearsci.2020.103940

[9] Pham, L, T., Oksum, E., & Do TD. (2019). Edge enhancement of potential field data using the logistic function and the total horizontal gradient. Acta Geodaetica et Geophysica 54:143–155

[10] Alvandi, A., Toktay, H, D., & Nasri, S. (2022a). Application of direct source parameter imaging (direct local wave number) technique to the 2D gravity anomalies for depth determination of some geological structures. Acta Geophys. . https://doi.org/10.1007/s11600-022-00750-6.

[11] Salem, A., Simon, W., Fairhead, J. D., Ravat, D. & Smith, R. (2007). Tilt-depth method: A simple depth estimation method using -order magnetic derivatives. The Leading Edge, 26(12), 1502-1505.

[12] de Souza, J., & Ferreira, F. J. F.(2015). The application of the Signum transform to the interpretation of magnetic anomalies. ASEG-PESA 2015, Geophysics and Geology together for Discovery, 24th International Geophysical Conference and Exhibition, Expanded Abstracts.

[13] Castro, F, R., Oliveira, S, P., De Souza, J., &Ferreira, FJF. (2018). GRAV-MAG SUITE: an open source MATLAB-based program for processing potential field data. VIII Simpósio Brasileiro de Geofísica. Pará, Brazil: Brazilian Geophysical Society.

[14] Cooper, G. R. J.(2015). Using the analytic signal amplitude to determine the location and depth of thin dikes from magnetic data: Geophysics, 80(1): J1-J6.

[15] Prasad, K.N.D., Pham, L.T. & Singh, A.P. (2022). A Novel Filter "ImpTAHG" for Edge Detection and a Case Study from Cambay Rift Basin, India. Pure and Applied Geophysics, 179 (6), 2351-2364.

[16] Alvandi, A., Toktay, H, D., & Pham, L, T. (2022c). Interpretation of gravity data using logistic function and total horizontal gradient (LTHG) – A case study: Charak anticline, 7 (4), 401-412.

[17] Razavi, S.A. & Jafari, F., (2008) Potash exploration via magnetometry and gravity methods in AjiChai (East Azerbaijan) and Ghareh-Aghaj (Zanjan Province). A Report in Geological Survey of Iran. pp: 75 (Persian).

[18] Abedi, M. (2018). An integrated approach to evaluate the Aji-Chai potash resources in Iran using potential field data. Journal of African Earth Sciences, (139), 379-391.

[19] Maghsoudi, M. (2021). Desert Landscapes and Landforms of Iran, Geography of the Physical Environment, https://doi.org/10.1007/978-3-030-58912-7_7.

[20] Toktay, H. D. & Alvandi, A. (2021). Application of the analytic signal amplitude and the Bott-Smith formula as a simple and very fast depth determination method of gravity anomalies: Application on synthetic and field profile data. Journal of Indian Geophysical Union, 25, 9-19.

[21] Reid, A B, Allsop, J M, Granser, H, Millet A J and Somerton, I W 1990. Magnetic interpretation in three dimensions using Euler deconvolution, Geophysics, 55, 80–91.

[22] Thompson, D. T. 1982, EULDPH: A new technique for making computer-assisted depth estimates from magnetic data, Geophysics, 47, 31–37.

[23] Abtahi SM, Pedersen LB, Kamm J, Kalscheuer T. A New Reference Model for 3D Inversion of Airborne Magnetic Data in Hilly Terrain - A Case Study fromNorthern Sweden. Geophysics (2018) 83:B1–B12. doi:10.1190/geo2016-0331.1